Monthly Notices
of the
ROYAL ASTRONOMICAL SOCIETY

MNRAS **461,** L26–L31 (2016)
Advance Access publication 2016 March 28

doi:10.1093/mnrasl/slw054

A recent strong X-ray flaring activity of 1ES 1959+650 with possibly less efficient stochastic acceleration

B. Kapanadze,[1,2]★† D. Dorner,[3] S. Vercellone,[2] P. Romano,[2] S. Kapanadze[1] and T. Mdzinarishvili[1]

[1]*E. Kharadze Abastumani Astrophysical Observatory, Ilia State University, Colokashvili Av. 3/5, 0162 Tbilisi, Georgia*
[2]*INAF, Istituto di Astrofisica Spaziale e Fisica Cosmica, Via U. La Malfa 153, I-90146 Palermo, Italy*
[3]*Universität Würzburg, Institute for Theoretical Physics and Astrophysics, Emil-Fischer-Str. 31, D-97074 Würzburg, Germany*

Accepted 2016 March 22. Received 2016 March 22; in original form 2016 February 22

ABSTRACT

We present an X-ray flaring activity of 1ES 1959+650 in 2015 August–2016 January, which was the most powerful and prolonged during the 10.75 yr period since the start of its monitoring with X-ray Telescope onboard *Swift*. A new highest historical 0.3–10 keV count rate was recorded three times that makes this object the third BL Lacertae source exceeding the level of 20 counts s^{-1}. Along with the overall variability by a factor of 5.7, this epoch was characterized by fast X-ray flares by a factor of 2.0–3.1, accompanied with an extreme spectral variability. The source also shows a simultaneous flaring activity in the optical – UV and 0.3–100 GeV bands, although a fast γ-ray flare without significant optical – X-ray counterparts is also found. In contrast to the X-ray flares in the previous years, the stochastic acceleration seems be less important for the electrons responsible for producing X-ray emission during this flare that challenges the earlier suggestion that the electrons in the jets of TeV-detected BL Lacertae objects should undergo an efficient stochastic acceleration resulting in a lower X-ray spectral curvature.

Key words: BL Lacertae objects: individual: 1ES 1959+650.

1 INTRODUCTION

BL Lacertae objects (BLLs) are widely accepted to be active galactic nuclei (AGNs) with a relativistic jet closely aligned with the line of sight that is successfully explaining their prominent features like a non-thermal continuum emission across the whole spectrum, and strong flux variability in all spectral bands (Massaro, Paggi & Cavaliere 2011a). The spectral energy distributions (SED) of BLLs show the presence of two broad components. The lower frequency one is widely accepted to be due to synchrotron radiation emitted by relativistic electrons in the jet, while an inverse Compton (IC) scattering of synchrotron photons by the same electron population should produce the higher-frequency bump (so-called synchrotron self-Compton mechanism, SSC), although the alternative scenarios are also proposed (see Krawczynski et al. 2004). We can draw conclusions about the validity of these models via the study of flux variability character in different spectral bands and their cross-correlations, which, on their turn, yield very important clues about the physics, the structure and the dynamics of a BLL emission zone.

Here, we report a strong X-ray flaring activity of the TeV-detected BLL 1ES 1959+650 ($z = 0.047$), observed with X-ray Telescope (XRT; Burrows et al. 2005) onboard the *Swift* satellite (Gehrels et al. 2004) during 2015 August–2016 January, which was significantly stronger and prolonged compared to those reported by (Kapanadze et al. 2016, hereafter K16), Aliu et al. (2013), Tagliaferri et al. (2008) etc. from the X-ray observations performed during 2000–14.

2 OBSERVATIONS AND DATA REDUCTION

The XRT data were processed with the XRTDAS package developed at the ASI Science Data Center (ASDC) and distributed by HEASARC within the HEASOFT package (v. 6.16). They were reduced, calibrated and cleaned by means of the XRTPIPELINE script using the standard filtering criteria and the calibration files of *Swift* CALDB (20150721). The extraction of the 0.3–10 keV light curves and spectra from the Windowed Timing (WT) and Photon Counting (PC) observations, as well their correction on different effects was performed in the same way described in detail in K16. The photometry for the sky-corrected images obtained in all UVOT bands was performed via the HEASOFT task UVOTSOURCE and the calibration files included in the CALDB. The measurements were performed using the 5 arcsec radius source aperture for *V, B, U* bands, and the 10 arcsec radius – for *UVW1*, *UVM2*, *UVW2* bands to take properly into account

★ E-mail: bidzina_kapanadze@iliauni.edu.ge
† Guest scientist at Astronomy Department, University of Michigan

Table 1. Extract from the summary of the *Swift*–XRT observations. The columns (3) and (4) give the exposure time (in seconds) and the mean 0.3–10 keV count rate with its error in the brackets for the given ObsID (in counts s^{-1}), respectively; Column (5) – the value of χ^2 with corresponding d.o.f for the particular observation.

ObsID (1)	Obs. Start – End (UTC) (2)	Exp. (3)	Count Rate (4)	χ^2/d.o.f. (5)
00035025149	2015-08-01 22:20:58 08-01 23:22:22	550	10.08(0.26)	9.9/8
00035025151	2015-08-15 11:49:58 08-15 14:10:17	959	7.50(0.10)	33.6/14

Table 2. Extract from the results of the *Swift*–UVOT observations. The flux values in each band are given in units of mJy.

	V		*B*		*U*		*UVW1*		*UVM2*		*UVW2*	
ObsId	Mag.	Flux	Mag.	Flux	Mag.	Flux	Mag.	Flux	Mag.	Flux	Mag.	Flux
35025149	14.54(0.06)	5.60(0.30)	14.94(0.04)	4.29(0.17)	14.06(0.04)	3.44(0.16)	14.02(0.05)	2.21(0.12)	13.77(0.06)	2.38(0.18)	13.88(0.05)	2.07(0.10)
35025151	14.42(0.06)	6.25(0.36)	14.74(0.04)	5.15(0.21)	13.94(0.05)	3.84(0.18)	13.79(0.06)	2.73(0.15)	13.67(0.06)	2.61(0.14)	13.57(0.05)	2.75(0.13)

wider PSFs. The magnitudes were then corrected for the Galactic absorption and converted into linear fluxes (in mJy) following the recipe provided in K16.

We extracted the 300 MeV–100 GeV photon fluxes from the *Fermi*-LAT observations. The events of the diffuse class were used from a region of interest (ROI) of the 10 degrees radius, centred on the coordinates of 1ES 1959+650, and processed with the Fermi Science Tools package (version v10r0p5) with P8R2_V6 instrument response function. The cuts on the zenith angle (>100 deg) and on the spacecraft's rocking angle (>52 deg) were applied. A background model including all γ-ray sources from the *Fermi*–LAT 4-year Point Source Catalog (3FGL, Acero et al. 2015) within 20 deg of 1ES 1959+650 is created. The spectral parameters of sources within the ROI are left free during the minimization process, while those outside of this range were held fixed to the catalogue values. The Galactic and extragalactic diffuse γ-ray emission as well as the residual instrumental background are included using the recommended model files.

During August 2–December 10 2015, the source was observed at TeV energies for 151.8 h (distributed over 96 nights) with the First G-APD Cherenkov Telescope (FACT; Anderhub et al. 2013) located in Observatorio del Roque de los Muchachos (La Palma, Spain). The FACT Collaboration provides the results of a preliminary quick-look analysis on http://www.fact-project.org/monitoring. These background-subtracted light curves are not corrected for the effect of changing energy threshold with changing zenith distance and ambient light, and no data quality selection is done (Dorner et al. 2015). During the phase of the enhanced flux, 1ES 1959+650 was detected with more than 3σ in the three nights of 2015 October 18/19 (MJD 57313.8), November 15/16 (MJD 57341.8) and November 20/21 (MJD 57346.8).

3 RESULTS, DISCUSSION AND CONCLUSIONS

3.1 Timing

The source was observed 52 times with XRT between 2015 August 1 and 2016 January 19, mostly in the framework of the Target of Opportunity (ToO) observations triggered by us. The information about each pointing and the measurement results are provided in Table 1.[1] The results of the UVOT observations are presented in Table 2 where the dereddened magnitudes and corresponding fluxes are provided for each band.

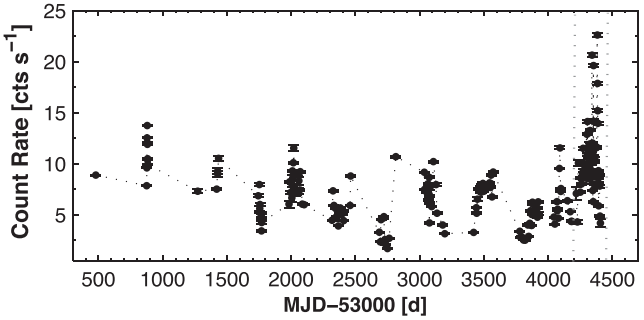

Figure 1. Long-term 0.3–10 keV light curve of 1ES 1959+650 from the *Swift*–XRT observations performed between 2005 April 19 and 2016 January 19. Its part, corresponding the campaign starting since 2015 August 1, is included within vertical dashed lines.

From Fig. 1, we see that the source underwent a significantly stronger X-ray flare in 2015 August–2016 January compared to those observed in the past years. During this period, the 0.3–10 keV count rate varied by a factor of 5.7 with the maximum value $F^{\rm max}_{0.3-10\,{\rm keV}} = 23.0 \pm 0.2$ counts s^{-1} (see Fig. 2a, upper panel) that makes 1ES 1959+650 the third BLL brighter than 20 counts s^{-1} (after Mrk 421 and Mrk 501). While the weighted mean count rate during 2005 April–2015 July was 5.87 ± 0.01 counts s^{-1}, this quantity amounted to 9.72 ± 0.02 counts s^{-1} in 2015 August–2016 January. In this case, the source was brighter than 10 counts s^{-1} during 46 per cent of all observations. Note that 1ES 1959+650 was brighter than this threshold only 12 times during the 133 XRT observations in the past 10.3 yr. Furthermore, while the higher X-ray brightness states mostly lasted a few weeks during the flaring activities seen in 2005–14 (see K16), the source remained bright for almost 5.5 months in the case of the here presented campaign. Although the source showed its higher X-ray brightness state during about 4 months in 2013 July–October (see K16), there was a gap of 45 d in the middle of that period, and it may have had a lower state in this interval. Furthermore, the maximum 0.3–10 keV count rate was only 9.2 counts s^{-1} during that event.

During the recent flaring activity, the new highest historical observation-binned count rates of 14.35 ± 0.42, 20.55 ± 0.18 and 22.95 ± 0.16 counts s^{-1} were recorded on MJD 57332.1, MJD 57341.9 ('Event 1'), MJD 57382.8 ('Event 2'), respectively. The last two events were related to the fast flares by a factor of 3.1

[1] The full versions of Tables 1, 2 and 5 are available online. Table 4 is completely included in the online material.

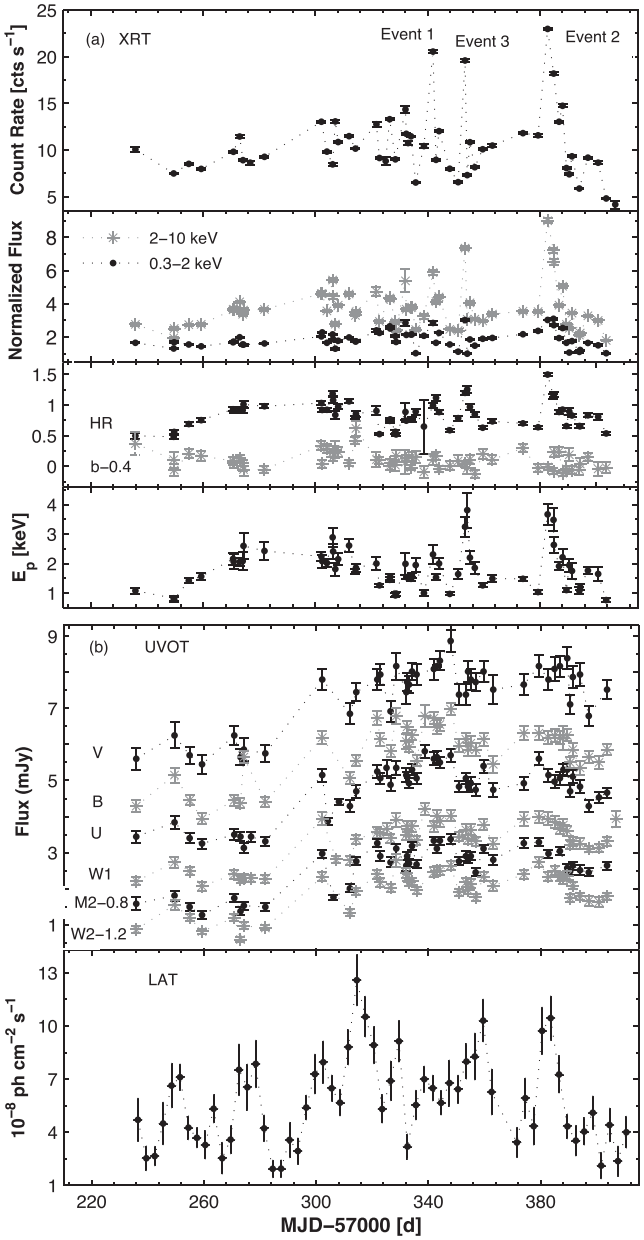

Figure 2. (a) The 0.3–10 keV light curve from the 2015 August 1–2016 January 19 period along with those constructed via the unabsorbed 0.3–2 keV and 2–10 keV model fluxes normalized to their minimum values in the particular period (second panel, the 2–10 keV plot is shifted arbitrarily for a better resolution), *HR* and curvature parameter (third panel), $E_{\rm p}$ (lower panel) versus time; (b) light curves from UVOT and LAT 0.3–100 GeV bands (upper and lower panels, respectively). The latter light curve is constructed using the 3 d bins.

and 2.0 in 6.2 and 3.4 d, respectively. Another fast flare by a factor of 3.0 in 2.45 d was centred on MJD 57353.35 when the 0.3–10 keV count rate reached the value of 19.60 ± 0.15 counts s^{-1} ('Event 3'). It was followed by a decay by a factor of 2.7 in 0.75 d. Events 1 was also characterized by a very fast decay by a factor of 2.3 in 1.05 d. The fastest flux doubling and halving times were 1.55 and 0.53 d, respectively, calculated as $\tau_{\rm d,\,h} = \Delta t \times \ln(2)/\ln(F_2/F_1)$ (Saito et al. 2013). Event 1 coincides with one of the detections of 1ES 1959+650 with a 3σ significance by FACT. The source was also detected by VERITAS at the $(26–30)\sigma$ level and the VHE flux above 200 GeV was 0.45–0.50 Crab on MJD 57303 and MJD 57304 (Mukherjee et al. 2015).

From the past X-ray campaigns, a larger flux variability was reported only by Krawczynski et al. (2004) when the 10 keV flux decreased by a factor of 18.7 in 4 weeks in the epoch consisting of the prominent ' orphan' TeV-flare on 2002 June 4.

The second panel of Fig. 2(a) also shows a timing behaviour of the unabsorbed soft 0.3–2 keV and hard 2–10 keV fluxes. We see that they mostly followed each other, and that was reflected in a strong correlation between them, presented in Fig. 3a (see Table 3 for the corresponding Pearson correlation coefficient and *p*-value). However, the hard flux showed a significantly stronger variability compared to the soft one – $F_{\rm var} = 46 \pm 1$ per cent for the 2–10 keV band as opposed to 28 ± 1 per cent for the soft X-rays. This fact is especially evident for Event 2 when the hard flux increased by a factor of 3, while the 0.3–2 keV flux increased only 1.3-times, causing a shift of synchrotron SED peak location by 2.64 keV and spectral hardening corresponding to the drop of the parameter *a* by 0.43 and the increase in the hardness ratio (*HR*) by 0.859.

The light curves from all UVOT bands show a variability by a factor of 1.6–2.2 (progressively stronger to higher frequencies) and the presence of prolonged higher optical – UV states since MJD 57302 (Fig. 2b, upper panel). However, the higher states in all UVOT bands were observed in past years (in contrast to the XRT and LAT bands; see K16).

In 2015 August – 2016 January, the 0.3–100 GeV flux was mostly higher than 4×10^{-8} ph cm^{-2} s^{-1} from the 2 weeks-binned data that happened only very few times during 2008–14 (see K16 and Aliu et al. 2013). It was always detectable with 3σ significance from the 3 d-binned data while the source detection was mainly below this threshold before 2015 August 1. The corresponding light curve shows a flaring activity by a factor of 2.8–6.5 (Fig. 2b, lower panel). One of the flares coincided with Event 2 and, an increasing γ-ray activity was seen in the epoch of Event 3, although the strongest flare with the highest γ-ray state was recorded around MJD 57314 (along with the 3σ detection by FACT on this day) when no significant optical – X-ray variability was seen (Fig. 2b). Therefore, this event may be considered as another possible 'orphan' γ-ray flare in this source, in addition to those reported in Krawczynski et al. (2004) and K16. However, the *Swift* observations were relatively sparse in this epoch, and we cannot exclude the occurrence of a fast X-ray flare during the days with no UV–X-ray data. Therefore, this result should be considered with a caution.

We have revealed six cases of intraday X-ray flux variability (IDV) with 99.9 per cent confidence using the χ^2-statistics and seven cases with 99.5 per cent confidence (so-called possible variability; Andruchow, Romero & Cellone 2005). These events are characterized by the fractional rms variability amplitude $F_{\rm var}$ of 3–45 per cent (calculated according to Vaughan et al. 2003; see Table 4, online). The fastest events observed within 1 ks interval are presented in Fig. 4 (all of them are detected with 99.5 per cent confidence). A flux increase by 30 per cent within 240 s was observed during the first orbit of the observation performed on 2015 November 2 (Fig. 4a). Note that this event was a part of the longer IDV detected with 99.9 per cent confidence (including the second orbit of this observation separated by about 18 h from the first one). A successive drop by 18 per cent and increase by 23 per cent within 360 s was recorded on 2015 October 11 (Fig. 4b). In contrast to this event, a flux increase by 25 per cent in 180 s was followed by a drop by 34 per cent during the next 240 s interval on 2016 January 7

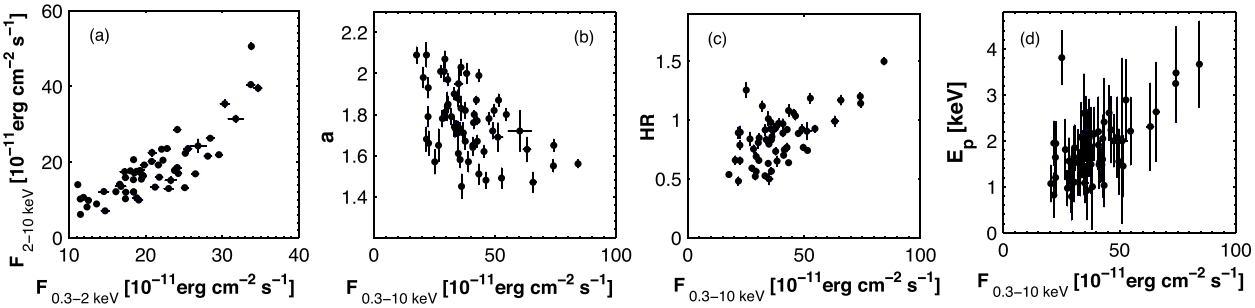

Figure 3. Correlation between different spectral parameters and fluxes.

Table 3. Correlations between different spectral parameters and multiband fluxes.

Quantities	r	p
$F_{0.3-2\,\mathrm{keV}}$ and $F_{2\text{-}10\,\mathrm{keV}}$	0.74(0.05)	7.14×10^{-13}
a and $F_{0.3-10\,\mathrm{keV}}$	−0.40(0.11)	1.35×10^{-4}
HR and $F_{0.3-10\,\mathrm{keV}}$	0.55(0.08)	2.60×10^{-6}
E_p and $F_{0.3-10\,\mathrm{keV}}$	0.45(0.12)	7.51×10^{-5}

(Fig. 4c). In the case of the 2015 October 27 pointing, a flux fluctuation by 10–20 per cent within 840 s was observed (Fig. 4d). As for the IDVs with 99.9 confidence, they occurred during the observations consisting of two orbits separated by 1–23 h from each other. The most extreme variability was observed on 2015 November 24 when the 0.3–10 keV count rate dropped by a factor of 2.3 in about 18 h (during the decreasing phase of Event 3). Note that the source also showed IDVs = within 1 ks in past years (see K16), but these events were more extreme in the here presented period.

3.2 Spectra

For each *Swift*–XRT observation, we performed the spectral analysis by fixing the absorbing Hydrogen column density N_H to the Galactic value of 1.00×10^{21} cm^{-2} (Kalberla et al. 2005), and using the log-parabolic model (LP; Massaro et al. 2004)

$$F(E) = K(E/E_1)^{-(a+b\log(E/E_1))} \quad \mathrm{ph\ cm^{-2}\ s^{-1}\ keV^{-1}}, \qquad (1)$$

with E_1 – the reference energy, fixed to 1 keV (a) the photon index at 1 keV; (b) the curvature parameter; K – the normalization factor. The results of the spectral analysis performed with the LP model are provided in Table 5. The HR is calculated as a ratio of unabsorbed 2–10 keV to 0.3–2 keV flux. In Table 6, we present the properties of the distribution of the parameters a, HR, b. For a comparison, we have included the same data for 1ES 1959+650 from the 2005–14 period.

Generally, this source showed highly curved spectra compared to the 2005–14 period (see Fig. 5 presenting the LP fit with the spectrum extracted from the XRT observation of 2015 October 19. The residuals show a good agreement between the model and the experimental data). About 73 per cent out of the values of the parameter b are higher than $b = 0.40$ from their broad range $\Delta b = 0.74$. The maximum value b_max is by $\Delta b = 0.35$ larger, and the distribution peak is shifted by 0.14 towards higher values compared to the spectra reported in K16. In contrast to the 2005–14 period, the parameter b does not show an anticorrelation with the unabsorbed 0.3–10 keV flux (see Fig. 2a where b is plotted versus time) which, in combination with the fact that most of spectra exhibited $b \sim 0.3$, led K16 to the suggestion about the importance of stochastic acceleration of the emitting electrons nearby the shock front moving through the jet. The absence of this anticorrelation and significantly stronger curved spectra may indicate that the stochastic mechanism was less favoured during the here presented flare, in contrast to those observed during 2005–14, and this fact challenges the suggestion of Massaro et al. (2011a) that the electrons in the jets of TeV detected BLLs (including 1ES 1959+650) should undergo a more efficient stochastic acceleration resulting in broad synchrotron SEDs ($b \sim 0.3$) than in TeV-undetected ones with $b \sim 0.7$. Note that similar high curvatures have been rarely reported also for other TeV-detected BLLs (see e.g. Massaro et al. 2004, 2008; Kapanadze et al. 2014). However, the X-ray flares from the 2005–14 period were sampled very sparsely, which makes it impossible to study a distribution of the parameter b per flare, and compare them to that from the 2015 August–2016 January period via the parameter $D_\mathrm{K-S}$ (distance between the distributions to be compared) and check the significance of the Kolmogorov–Smirnov (K–S) test by means of the method based on the Monte Carlo simulations (Massaro, Harris & Cheung 2011b). Furthermore, the maximum and minimum flux

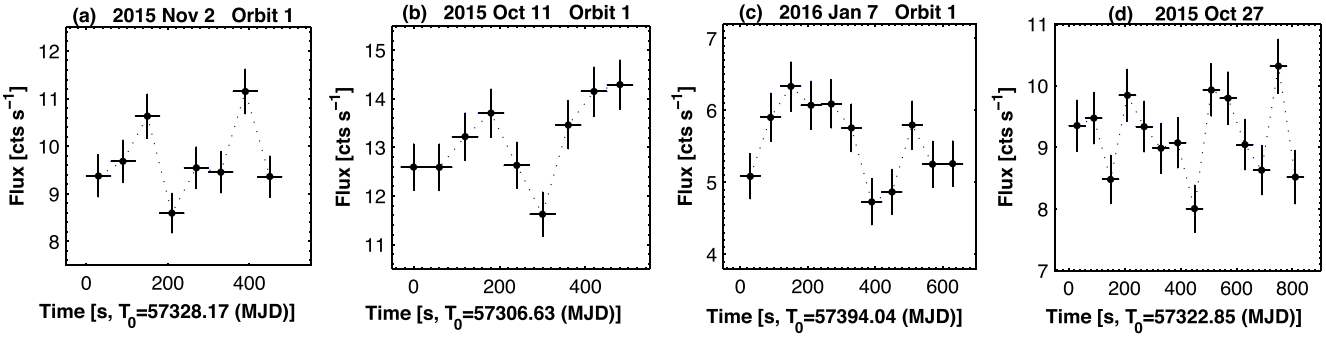

Figure 4. The 0.3–10 keV light curves from the observations with IDVs at the 99.5 per cent confidence.

Table 5. Extract from the summary of the XRT spectral analysis with LP model. The E_p values (Column 4) are given in keV; the parameter K (Column 5) is given in units of 10^{-2}; unabsorbed 0.3–2, 2–10 and 0.3–10 keV fluxes (Columns 7–9) – in erg cm^{-2} s^{-1}.

ObsId (1)	a (2)	b (3)	E_p (4)	K (5)	χ^2/d.o.f. (6)	log $F_{0.3-2\,keV}$ (7)	log $F_{2-10\,keV}$ (8)	log $F_{0.3-10\,keV}$ (9)	HR (10)
35025149	1.95(0.09)	0.77(0.19)	1.08(0.10)	6.42(0.14)	48.2/54	−9.986(0.021)	− 10.288(0.039)	−9.809(0.021)	0.499(0.051)
35025151 Orbit1	2.09(0.06)	0.51(0.13)	0.82(0.10)	6.51(0.14)	92.5/86	−9.832(0.016)	− 10.15(0.029)	−9.662(0.015)	0.481(0.037)

Table 6. Distribution of different spectral parameters.

	2015 August–2016 January				2005–14			
Par.	Min.	Max.	Peak	σ^2	Min.	Max.	Peak	σ^2
b	0.28	0.98	0.49	0.021	0.18	0.67	0.35	0.010
a	1.45	2.09	1.74	0.028	1.76	2.37	2.02	0.016
HR	0.481	1.496	0.845	0.043	0.317	0.918	0.550	0.013

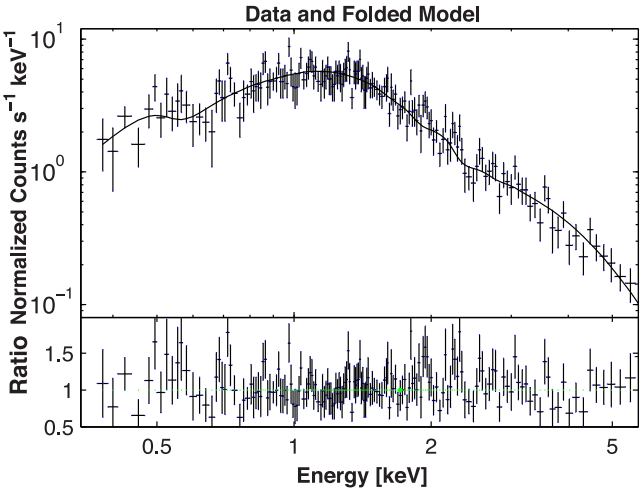

Figure 5. The spectrum from Orbit 2 of the XRT observation performed on 2015 October 19, fitted with the LP model (upper panel), and the distribution of the residuals (lower panel).

levels varied significantly from flare to flare in 2005–14, and a very sparse sampling of these events prevents us from firmly distinguishing the observations corresponding to quiescent and flaring states, and constructing the distribution of the parameter b jointly for the X-ray flares observed in past years. Note that the distribution of the parameter b presented in K16 consists of the values from all XRT observations of 1ES 1959+650 in 2005–14, and the use only those from the flaring epochs (i.e. the removal of higher values of the parameter b from the sample, since it showed an anticorrelation with the flux) would shift the median value of the distribution towards lower curvatures that, on its turn, would make this distribution more different from that observed in 2015 August–2016 January period. Moreover, there are other possibilities that would result in a change of the curvature of the synchrotron spectrum, e.g. a radiative cooling evolution (Massaro et al. 2006). Due to these reasons, the aforementioned suggestion about the less effective stochastic acceleration during the here presented flare should be treated with a caution. We have not found a positive correlation between the parameters a and b, predicted for the case of the prominence of energy-dependent acceleration probability process (EDAP) at the shock front (Massaro et al. 2004).

The parameter a also showed a wide range of the values $\Delta a = 0.54$ whose 49 per cent are lower than $a = 1.76$ corresponding to the hardest 0.3–10 keV spectrum from the 2005–14 period (K16). Fig. 3b shows a moderate anticorrelation between a and 0.3–10 keV model flux, revealing that the source mainly followed a 'harder-when-brighter' trend. The latter is also evident from Fig. 2a, presenting the variability of the parameter HR, and from Fig. 3c with a positive correlation between HR and the 0.3–10 keV flux. Note that 19 per cent of the spectra show $HR > 1.00$ that never has happened in the past.

The location of the synchrotron SED peak, calculated as $E_p = E_1 10^{(2-a)/2b}$ keV, also shows a very wide range between 0.76 ± 0.10 keV and 3.81 ± 0.60 keV, and their 36 per cent are greater than 2 keV that never have been reported for this source. For example, $E_p^{max} = 1.84$ keV and the 38 per cent of the spectra showed E_p <0.80 keV (which should be considered as upper limits to the intrinsic value of E_p; see K16) in 2005–14. Although the presence of the synchrotron SED peak above 10 keV was stated by Krawczynski et al. (2004) for some observations during the extreme variability in 2002, that spectral study was carried out in the 3–25 keV band using the simple powerlaw, and the presence of the synchrotron SED peak beyond 10 keV was concluded from the fact that the 3–25 keV photon index was below the value $\Gamma = 2$, and no calculations of the E_p values were performed. This parameter shows a positive correlation with the 0.3–10 keV flux (Fig. 3d). From Fig. 2a, we see that the synchrotron SED peak mainly moved towards higher frequencies with an increasing flux and vise versa. The highest values of this parameter belong to the epochs of Events 2,3 when shifts by $\Delta E_p = 2.65$–2.85 keV occurred. A similar trend for 1ES 1959+650 was also reported in Tagliaferri et al. (2003) and K16.

Only one spectrum (from the observation of 2015 September 11) was fitted well with a simple power-law model, given by $F(E) = KE^{-\Gamma}$, with the photon index throughout the observation band Γ, equal to 1.95 ± 0.4 in this case.

We conclude that 1ES 1959+650 is one of the most extreme BLLs with a complex, unpredictable timing/spectral variability, exclusively strong and prolonged X-ray flares in some epochs, 'orphan' γ-ray events. Further, more densely sampled X-ray observations would be very important to draw firm conclusions about the relevance of stochastic mechanism in the acceleration of the X-ray emitting particles.

ACKNOWLEDGEMENTS

BK, SK and TM thank Shota Rustaveli National Science Foundation and Ilia State University for the grant FR/377/6-290/14. PR acknowledges the contract ASI-INAF I/004/11/0. BK thanks the *Swift* PI, Neil Gehrels for approving his requests for the ToO observations. This research has made use of the XRTDAS software, developed under the responsibility of the ASDC, Italy. We thank the FACT Collaboration for providing their analysis results publicly available. Finally, we thank the anonymous referee for his/her very useful comments and suggestions that helped to improve the quality of the Letter.

REFERENCES

Acero F. et al., 2015, ApJS, 218, 23
Aliu E. et al., 2013, ApJ, 775, 3
Anderhub H. et al., 2013, J. Instrum., 8, P06008
Andruchow I., Romero G. E., Cellone S. A., 2005, A&A, 442, 57
Burrows D. N. et al., 2005, Space Sci. Rev., 120, 165
Dorner D. et al., 2015, preprint (astro-ph/1502.02582)
Gehrels N. et al., 2004, ApJ, 611, 1005
Kalberla P. M. W., Burton W. B., Hartmann Dap., Arnal E. M., Bajaja E., Morras R., Pppel W. G. L., 2005, A&A, 440, 775
Kapanadze B., Romano P., Vercellone S., Kapanadze S., 2014, MNRAS, 444, 1077
Kapanadze B., Romano P., Vercellone S., Kapanadze S., Mdzinarishvili T., Kharshiladze G., 2016, MNRAS, 457, 704 (K16)
Krawczynski H. et al., 2004, ApJ, 601, 151
Massaro E., Perri M., Giommi P., Nesci R., 2006, A&A, 413, 489
Massaro E., Tramacere A., Perri M., Giommi P., Tosti G., 2006, A&A, 448, 861
Massaro F., Tramacere A., Cavaliere A., Perri M., Giommi P., 2008, A&A, 478, 395
Massaro F., Paggi A., Cavaliere A., 2011a, ApJ, 742, L32
Massaro F., Harris D. E., Cheung C. C., 2011b, ApJS, 197, 24
Mukherjee R., 2015, Astron. Telegram, 8148
Saito S., Stawarz Ł., Tanaka Y. T., Takahashi T., Madejski G., D'Ammando F., 2013, ApJ, 766, L11
Tagliaferri G., Ravasio M., Ghisellini G., Tavecchio F., Giommi P., Massaro E., Nesci R., Tosti G., 2003, A&A, 412, 711
Tagliaferri G. et al., 2008, ApJ, 679, 1029
Vaughan S., Edelson R., Warwick R. S., Uttley P., 2003, MNRAS, 345, 1271

SUPPORTING INFORMATION

Additional Supporting Information may be found in the online version of this Letter:

Table 1. The summary of the *Swift*-XRT observations. The columns (3) and (4) give the exposure time (in seconds) and the mean 0.3 - 10 keV count rate with its error in the brackets for the given ObsID (in cts s-1), respectively; (5) - the value of χ^2 with corresponding dof for the particular observation.

Table 2. The results of the *Swift*-UVOT observations. The flux values in each band are given in units of mJy.

Table 4. The summary of the IDVs revealed with 99.9 and 99.5 per cent confidences from the XRT observations performed during 2015 August 1 - 2016 January 19. Column 2 gives a total extent of the observation consisting of the particular event, including the time intervals between two orbits of this observation (in hours).

Table 5. The summary of the XRT spectral analysis with log-parabolic model. The E_p values (Column 4) are given in keV; unabsorbed 0.3 – 2 keV, 2 – 10 keV and 0.3 – 10 keV fluxes (Columns 7 – 9) - in erg cm-2 s-1.
(http://www.mnrasl.oxfordjournals.org/lookup/suppl/doi:10.1093/mnrasl/slw054/-/DC1).

Please note: Oxford University Press is not responsible for the content or functionality of any supporting materials supplied by the authors. Any queries (other than missing material) should be directed to the corresponding author for the Letter.

This paper has been typeset from a TEX/LATEX file prepared by the author.